PAPER • OPEN ACCESS

Evolution of anisotropic distributions of weakly charged heavy ions downstream collisionless quasiperpendicular shocks

To cite this article: J A Kropotina *et al* 2018 *J. Phys.: Conf. Ser.* **1038** 012014

View the article online for updates and enhancements.

Related content

- Particular mechanism for continuously varying the compression ratio for an internal combustion engine
S Raiu, R Ctlinoiu, V Alexa et al.

- Pickup Ions at Termination Shock
Donald C. Ellison, Frank C. Jones and Matthew G. Baring

- Numerical studies of ion reflection in collisionless theta-pinch implosions using a hybrid Vlasov-fluid model
P.C. Liewer

IOP ebooks™

Bringing you innovative digital publishing with leading voices to create your essential collection of books in STEM research.

Start exploring the collection - download the first chapter of every title for free.

Evolution of anisotropic distributions of weakly charged heavy ions downstream collisionless quasiperpendicular shocks

J A Kropotina[1,2]**, A M Bykov**[1,2]**, A M Krassilchtchikov**[1] **and K P Levenfish**[1]

[1]Ioffe Institute, 194021, St. Petersburg, Russia
[2]Peter the Great St. Petersburg Polytechnic University, 195251, St. Petersburg

E-mail: `juliett.k@gmail.com`

Abstract. Hybrid simulations of quasiperpendicular collisionless shocks (QRCS) in multicomponent plasmas have revealed that weakly charged ions can keep anisotropic nonequilibrium distributions at relatively long distances downstream the shock front. However, analytic considerations suggest that such distributions lead to growth of the Alfven ion cyclotron (AIC) instability, which in turn governs isotropisation. Hence, we have conducted targeted hybrid simulations of QRCS with increased accuracy, which appeared to agree with the analytical predictions and suggest that the nonequilibrium distributions eventually relax due to the AIC instability. On another hand, downstream electromagnetic instabilities generated by anisotropic particle distributions may affect the energy balance, therefore influencing macroscopic shock parameters, such as the compression ratio. Simulations of QRCS with parameters close to those of the heliospheric termination shock measured by the Voyager mission, showed that an admixture of just 0.7% (by mass) of oxygen decreases the compression ratio by 3-4%. Thus, one might conclude that along with the effect of the pickup ions, the multi-species composition of the interplanetary plasma can add to the observed decrease of the shock compression.

1. Introduction

Shock waves provide a universal mechanism of conversion of kinetic energy of supersonic flows into the thermal energy of plasma, as well as into the energy of amplified magnetic fields and of suprathermal particles. In the strong enough collisionless shocks (typically, of a Mach number above a few depending on the shock obliquity) the electron resistivity cannot provide energy dissipation fast enough to create a quasi-steady shock transition on a microscopic scale [1–3]. The structure of the shock transition is governed by the instabilities of the ion flows and such shocks are called *supercritical*(see, e.g., [4]; [5]; [6]). At the microscopic scale the front of a supercritical shock is a transition region occupied by magnetic field fluctuations of an amplitude $\delta B/B \gtrsim 1$ and characteristic frequencies of about the ion gyro-frequency. Generation of the fluctuations is due to instabilities in the interpenetrating multi-flow ion movements. The width of the viscous transition region of a collisionless shock typically reaches a few hundred ion inertial lengths defined as $l_i = c/\omega_{\mathrm{pi}} \approx 2.3 \times 10^7\, n^{-0.5}$ cm. Here ω_{pi} is the ion plasma frequency and n is the ionized ambient gas number density measured in cm^{-3}. The width of the collisionless

shock transition region is smaller by many orders of magnitude than the Coulomb mean free path in the interstellar or intergalactic medium [7], so particle relaxation is due to collective electromagnetic field fluctuations. In such an enviroment nonequilibrium states can arise and be kept for distances much larger than the characteristic shock transition lengths. Particularly, quasi-stationary anisotropic velocity distributions of a small admixture of weakly charged heavy ions downstream QRCS (i.e., the shocks with initial magnetic field directed nearly transversely to the shock normal) were found by [8, 9] via hybrid plasma simulations.

Here we present a detailed modeling of AIC instability caused by such ion distributions. Due to the high nonlinearity of a collisionless shock and the strong coupling between electromagnetic fluctuations and the motions of charged particles, pure analytic studies of such processes are possible only in some special cases and still provide only approximate results. Hence we combine an analytic approach with numerical hybrid simulations of QRCS (see [8, 9] for more detailed discussions of this approach). In section 2 the hybrid code and initial parameters of a simulation are briefly described. In section 3 the resulting nonequilibrium distributions are shown and both analytical and numerical treatments of AIC instability are discussed, as well as their possible application of to the physics of the heliospheric termination shock.

2. Hybrid Simulations of Shocked Plasma Flows

A 3d second-order accurate particle-mesh hybrid code with exact magnetic field divergence conservation was used for simulations of QRCS evolution. The main feature of a hybrid code is that it combines hydrodynamic and particle-in-cell approaches, treating ions as particles and electrons as a neitralizing massless fluid ([10]). This allows one to self-consistently model processes governed by ions at time scales up to several thousand inverted ion gyrofrequencies (Ω_i^{-1}. A standard system of equations for a hybrid code is given in [11]. These equations are solved within a cyclic leapfrog approach with particle coordinates and velocities given at the odd timesteps and fields – at the even ones. A "Reconstruct-Solve-Average" algorithm including finite-volume discretisation, piesewise-parabolic reconstruction and linearized Roe-type Riemann solver (see, e.g., [12]) was implemented in the code to achieve the exact magnetic field divergence conservation. Triangular-shaped cloud representation of the ions and Boris particle pusher (see, e.g., [13]) were employed to move particles and calculate induced currents with second-order accuracy in time and space. The shock was initialized via the standard piston method, where a superalfvenic flow reflects from a conducting wall and forms the front moving oppositely to the initial flow.

3. Evolution of Heavy Ion Distributions
3.1. Nonequilibrium phase spaces and distributions
According to [8,9], nonequilibrium heavy ion distributions appear for various QRCS parameters, provided that the ion charge-to-mass ratio and relative density is low enough. For an illustrative example shown in Fig. 3.1 plasma parameters typical for a supernova reverse shock were chosen: the upstream Alfven Mach number (in the downstream frame) $M_A = 9.0$, the inclination angle (between the direction of the initial magnetic field and the shock normal) $\theta = 90^o$ (so the shock was exactly perpendicular), and the ratio of thermal to magnetic pressure $\beta = 1.0$. The reflecting wall was at $x = 0$, the initial flow moved to the left, and the initial number of model particles per cell (ppc) was equal to 200. Plasma consisted of 99% O IV and 1% Si II (by mass). Figure 3.1 shows the resulting phase spaces of the main element (left panels) and heavy ion admixture (middle panels) at $t = 100\Omega_i^{-1}$, where $\Omega_i = q_{main} B / m_{main} c$ is the main ions sort (O IV) gyrofrequency. The corresponding spatially averaged velocity distributions are given at the right panels. It is clear that while the main element phase spaces and distributions are isotropic and homogenious, the Si II ones show peculiar quasi-periodic structure, associated with heavy ions gyromotion downstream the shock. The averaged Si II velocity distributions

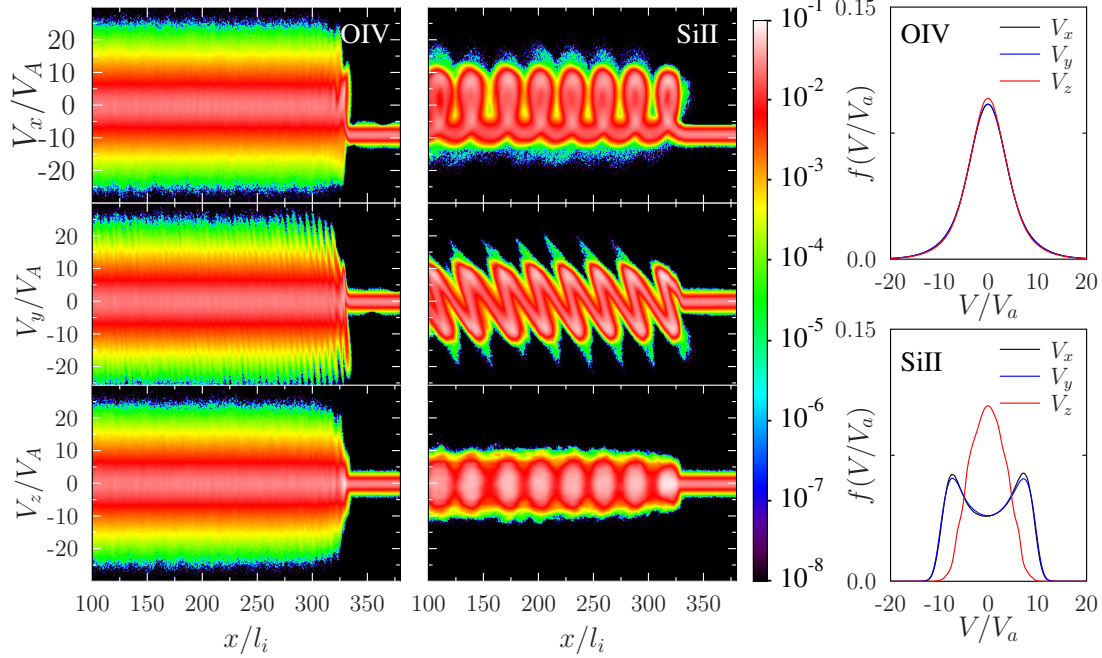are substantially anisotropic with preferred magnetic field direction (which is along z in this simulation).

Figure 1. The O IV and Si II $x - V$ phase spaces and velocities distributions in shock with $M_a = 9.0$, $\theta = 90^o$ and $\beta = 1.0$ at $t = 100\Omega_i^{-1}$. All lengths are given in the main element l_i, while velocities are in the far upstream $V_a = B_0/\sqrt{(4\pi\rho)}$.
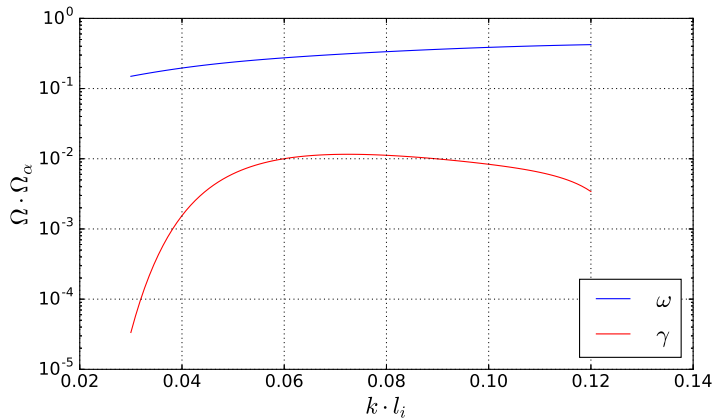

Figure 2. Solution of the dispersion equation for medium with macroscopic parameters and SiII distribution anisotropy taken from the simulated downstream region of the same shock as in figure 3.1. Positive γ indicate instability growth.

3.2. Alfven ion cyclotron instability

In paper [14] it was shown (with application to thermonuclear fusion) that temperature anisotropy of hot minority ions population with isotropic equilibrium background can drive the AIC instability, which leads to the hot minority distribution relaxation. In the kinetic

approach the distribution details appeared to be unimportant, so just the distribution moments are included in the following dispersion equation:

$$\Omega^2 - c^2 k^2 + \omega_{pe}^2 \frac{\Omega}{kV_{T\|e}} Z(\xi_e^{\pm}) + \omega_{pi}^2 \frac{\Omega}{kV_{T\|i}} Z(\xi_i^{\pm}) + \omega_{p\alpha}^2 \frac{\Omega}{kV_{T\|\alpha}} Z(\xi_\alpha^{\pm}) + \omega_{p\alpha}^2 (\frac{T_{\perp\alpha}}{T_{\|\alpha}} - 1)[1 + \xi_\alpha^{\pm} Z(\xi_\alpha^{\pm})] = 0$$

(1)

where $Z(\xi) = \pi^{-0.5} \int_{-\infty}^{\infty} dt \cdot exp(-t^2)/(t - \xi)$, $\xi_j^{\pm} = \Omega \pm \Omega_j/kV_{T\|j}$, $\Omega_j = q_j B/m_j c$, $\omega_{pj}^2 = 4\pi n_j q_j^2/m_j$ are jth species gyro- and plasma frequencies and $V_{T\|j}$, $T \| j$, $T_{\perp} j$ - their thermal velocities and temperatures with respect to the averaged magnetic field direction, i index corresponds to the main sort, while α - to the admixture. The solution of this equation (real and imaginary parts of Ω) is plotted versus k in Figure 3.1 for parameters and SiII anisotropy from model downstream region. The wave vector is given in inversed l_i and frequencies in Ω_α. It can be seen that there persists positive increment area, which means the instablity growth, though the maximum increment for such low SiII density is only $10^{-2}\Omega_\alpha$, which gives the characteristic growth time about $\tau \sim 500\Omega_i^{-1}$. In order to numerically confirm these analytical results we made the following test run of the hybrid code: one period of heavy ions phase space was placed in a periodic box with uniform averaged downstream magnetic field and equilibrium downstream main sort population. In order to avoid numerical effects and make visible the expected tiny AIC instability effect we increased number of ppc up to 2000. The resulting phase spaces and velocity distributions evolution for ppc=2000 are shown in Figure 3.2, while the space-averaged magnetic field variance evolution for cases of ppc=200 and ppc=2000 is given in Figure 3.2. It is clear that for the case ppc=200 numerical noise is greater than the effect we consider, while for ppc=2000 there can be seen even two instabilities. The first one grows up very rapidly and is substantially damped up to $t = 200\Omega_i^{-1}$. It gives rise to magnetic field fluctuations propagating along x axis, so it cannot be associated with AIC instability, which propagates along the averaged magnetic field direction (z in our case). Probably it is governed by heavy ions spatial inhomogenity, which was not included in analytic studies and is valuably reduced with time, as can be seen from Figure 3.2. The second, slowly growing, type of instability gives rise to magnetic field fluctuations, transverse to the magnetic field direction and propagating along it with nearly alfven speed. Its visible growth is roughly consistent with characteristic time $\tau \sim 500\Omega_i^{-1}$, obtained in kinetic theory approach. Figure 3.2 also indicates slow velocity distribution evolution towards isotropy. So it can be concluded that anisotropic heavy ion distributions drive AIC instability, which eventually leads to their relaxation on scales much less that Coulomb ones, but much greater than characteristic shock transition lengths.

3.3. Termination shock simulations
The effect of slow heavy ions temperature relaxation downstream QRCS leads to increased magnetic field fluctuations level in the vicinity of shock transition. This effect can therefore change the total energy balance and affect the Rankine-Hugonio relations. As Supernova remnant observations are indirect and cannot reveal such a local effect, we tested this hypothesis on the shock with parameters close to the Termination shock ones, measured by Voyager2 ([15]): $M_a = 4.0$ in downstream frame, $\theta = 82^o$, $\beta = 0.01$. Actual Solar wind composition includes about 85% of H II, 14.2% of He III and about 0.7% of heavier ions (by mass). So three test runs were done to estimate the heavy ions impact on the shock compression ratio: the first – for the pure Hydrogen shock, the second – for the shock consisting of H II and He III with Solar abundancies and the third one with admixture of 0.7% of O VII. For all cases the averaged downstream density was measured. The resulting values for the proton and proton-helium shocks coincided within the uncertainty, while addition of only 0.7% of O VII appeared to decrease the downstream density by 3-4%. The O VII distributions appeared to be anisotropic
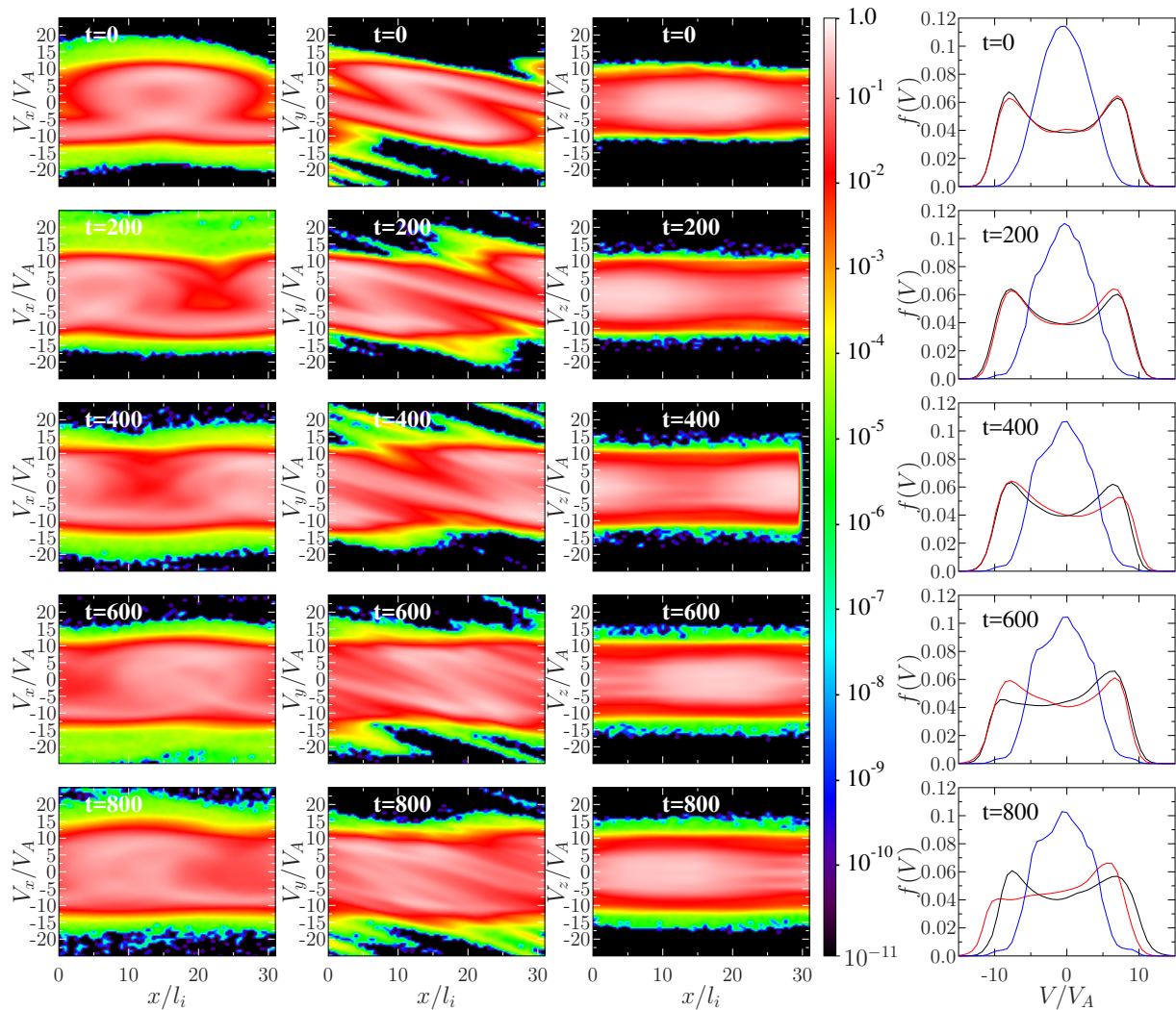
Figure 3. The O IV and Si II $x - V$ phase spaces and velocity distributions evolution in the test run(see text)

in the latter case, and the corresponding level of magnetic field fluctuations was higher than without Oxygen. This may lead to the conclusion that pickup ions are not the only reason of the observed low Termination shock compression ratio ([15]), but plasma composition can also affect this parameter. However, to check this statement, the full model including both pickup ions and heavy ions is needed, which is out of the scope of this paper.

4. Conclusions

The two approaches such as solution of plasma kinetic dispersion equation and hybrid modeling with increased number of particles per cell (ppc = 2000) follow to the same conclusion that anisotropic heavy ions distribution, arising downstream QRCS, lead to emerging of alfven ion cyclotron instability, which might grow rather slowly in case of small heavy ions relative density. Anyway, this instability has two consequences:

(i) Relaxation of anisotropic ion distributions to isotropic maxwellian ones on scales much less than the Coulomb length for typical astrophysical objects
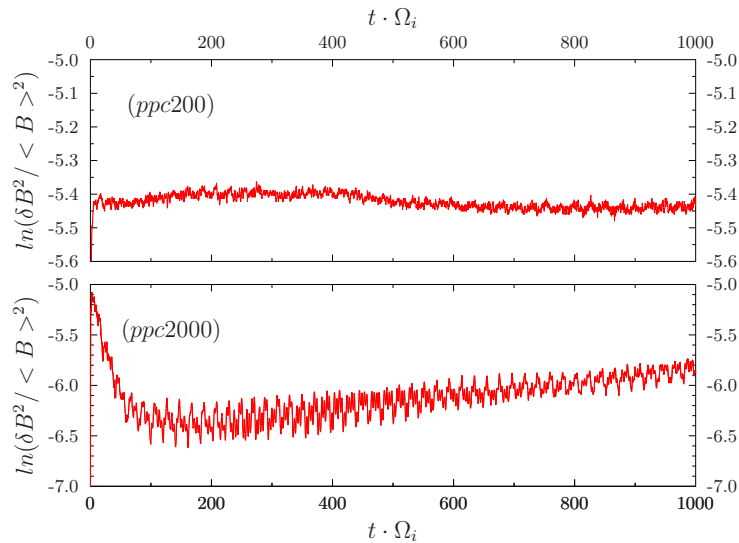
Figure 4. Relative magnetic field variance in the same run as in Figure 3.2

(ii) Increasing level of magnetic field fluctuations in the vicinity of transition, which can lead to changing of macroscopic shock parameters. The latter effect was illustrated on the example of the Termination shock.

5. Acknowledgements

References

[1] Sagdeev R Z 1966 *Reviews of Plasma Physics, New York: Consultant Bureau* vol 4 ed Leontovich M A pp 23–46
[2] Tidman D A and Krall N A 1971 *Shock waves in collisionless plasmas*
[3] Treumann R A 2009 *Astronomy and Astrophysics Reviews* **17** 409–535
[4] Kennel C F, Edmiston J P and Hada T 1985 *Washington DC American Geophysical Union Geophysical Monograph Series* **34** 1–36
[5] Lembege B and others/ 2004 *Space Science Reviews* **110** 161–226
[6] Burgess D *et al.* 2005 *Space Science Reviews* **118** 205–222
[7] Bykov A M, Paerels F B S and Petrosian V 2008 *Space Science Reviews* **134** 141–153 (*Preprint* 0801.1008)
[8] Kropotina and others Y A 2015 *Technical Physics* **60**(2) 231–239
[9] Kropotina and others Y A 2016 *Technical Physics* **61**(4) 517–524
[10] Winske D and Omidi N 1996 *JGR* **101** 17287–17304
[11] Matthews A P 1994 *J. Comput. Phys.* **112**(1) 102–116 ISSN 0021-9991
[12] R J LeVeque D Mihalas E D E M 2006 *Computational Methods for Astrophysical Fluid Flow* (Springer Science and Business Media)
[13] Birdsall C K and Langdon A B 1991 *Plasma Physics via Computer Simulation*
[14] Lashmore-Davies C N, Dendy R O and Kam K F 1993 *Plasma Physics and Controlled Fusion* **35** 1529–1540
[15] Richardson J D, Kasper J C, Wang C, Belcher J W and Lazarus A J 2008 *Nature* **454** 63–66